Efficient Wide-Band Evaluation of Mobile Communications Antennas Using $[Z]$ or $[Y]$ Matrix Interpolation with the Method of Moments

Kathleen L. Virga, *Senior Member, IEEE,* and Yahya Rahmat-Samii, *Fellow, IEEE*

***Abstract*—The development of novel antennas for mobile communications often relies on performance simulations. The evaluation of the antenna surface currents for many frequencies using the method of moments (MoM) can take a long time since the impedance matrix must be computed for each new frequency. This paper investigates and compares two efficient methods for the computation of the broad-band performance of mobile communications antennas using frequency interpolation of either the MoM impedance matrix [Z] or admittance matrix [Y]. In either method, the elements of only a few matrices at relatively large frequency intervals are directly computed. These matrices are then used to interpolate the elements of the respective [Z] or [Y] matrices at the intermediate frequencies. Both methods reduce the time it takes to compute the antenna performance over a wide frequency band. The implementation of each method to evaluate the performance of several different antennas used for mobile communications is discussed. Examples with both frequency-domain and time-domain results are presented and both near-field and far-field quantities are considered. The accuracy, the simulation run times, and the computational requirements of direct MoM, [Z] matrix interpolation, and [Y] matrix interpolation are compared.**

***Index Terms*— Broad-band antennas, helix, method of moments, mobile antennas, PIFA, [Y] matrix, [Z] matrix.**

I. Introduction

THE rapidly expanding personal and mobile communications services have necessitated the development of new antenna designs. An important task associated with the evaluation and comparison of antennas for these applications involves simulations to predict the antenna performance over a wide frequency range. A challenge in the design of such antennas is the development of advanced simulation software that allow the characterization of different configurations of perfect conducting wires and surfaces. Two popular electromagnetic analysis methods that are often applied to these class of antennas are the finite-difference time-domain (FDTD) [1], [2] and the surface-patch method of moments (MoM) [3]–[5].

Manuscript received June 2, 1997. This work was supported in part by Rockwell Science Center, Thousand Oaks, CA, and in part by the UC MICRO program.

K. L. Virga is with the Department of Electrical and Computer Engineering, University of Arizona, Tucson, AZ 85721 USA.

Y. Rahmat-Samii is with the University of California, Los Angeles, Los Angeles, CA 90095 USA.

Publisher Item Identifier S 0018-926X(99)02213-9.

FDTD predicts antenna performance over a wide band of frequencies in one simulation. A common FDTD formulation employs a three-dimensional (3-D) volumetric grid of uniform rectangular cells that results in a dense grid with small cells for radiators with detailed features. Geometries with curved and flared elements are approximated with a stairstep grid. A circular helix antenna, for example, must be approximated by an equivalent square helix [6] or requires a grid of extremely small stairstep cells to model the coil windings.

The frequency-domain MoM approach based upon the triangular patch surface model overcomes some of the geometrical modeling restrictions of FDTD. The MoM formulation can include a combination of wires of arbitrary shape attached to metallic surfaces of arbitrary shape. The triangular mesh allows curved and flared geometries to be modeled with a flat patch (or linear) surface approximation and allows detailed features to be modeled with a locally dense mesh. Piecewise linear wire elements allow coiled wires to be effectively modeled. The MoM approach computes the antenna performance one frequency at a time and requires the computation of many frequency points for broad-band performance evaluation or for short-pulse source antenna characterization. The computation over a wide frequency range can take a long time since the elements of the MoM $[Z]$ matrix must be recomputed for each new frequency point. Thus, techniques to minimize the computation time and significantly speed up the overall simulation process are highly desirable. Popular methods to reduce the computation time of MoM focus either on the use of numerical and geometrical approximations to quickly fill $[Z]$ or efficient matrix inversion and solution algorithms [7], [8].

Spatial interpolation methods used to efficiently fill the impedance matrix [9]–[11] have been studied. These approaches impose constraints on the structure of the surface mesh or the interpolation sampling criteria. A technique that employs the method of moments to compute rational function approximations for the transfer functions of antenna output performance parameters is discussed in [12]. This method is used to develop a compact transfer function of a single parameter, such as input impedance, over a broad frequency band. Since the transfer functions are determined for only one parameter at a time, they cannot be used to extract any additional information on the overall antenna performance. In [13], the Cauchy technique is used to calculate rational function approximations for the surface currents on a conducting

cylinder with a slit. These functions are used to extrapolate the broad-band response from narrow-band data. Since the functions represent currents, they must be recomputed for each different angle of incidence or excitation. The coefficients of the rational functions used in [12] and [13] can be determined either by many frequency samples of a response or the response and its higher order derivatives at a few frequencies. The derivatives are computed by actually modifying the MoM analysis program, which not only requires access to the source code, but can become rather difficult when complex basis or testing functions are used.

The present work focuses on implementing $[Z]$ matrix or $[Y]$ matrix interpolation methods that:

1) are easily implemented to an existing method of moments computer code, thus require no significant code modifications;
2) accurately construct the antenna surface currents, impedance, patterns, etc.;
3) utilize simple interpolation functions that require only a few coefficients;
4) apply to a wide variety of antenna configurations;
5) impose few restrictions on the antenna geometry modeling;
6) are independent of antenna excitation.

The $[Z]$ matrix and $[Y]$ matrix interpolation approaches discussed in this paper are outlined in Fig. 1. Both methods incorporate knowledge of the general frequency characteristics of the respective matrix elements in a way that reduces the time it takes to compute them at each frequency. The $[Z]$ matrix interpolation method was originally proposed by Newman and Forrai [14] for the scattering analysis of a microstrip patch. Newman [15] also used it for the impedance analysis of a straight dipole antenna and flat square plate. The present work expands the utilization of $[Z]$ matrix interpolation to the wide-band performance evaluation of complex antennas and also investigates a comparable $[Y]$ matrix interpolation approach. The methods are applied to the triangular surface-patch MoM formulation. The objective is to compare the versatility, accuracy, and computational efficiency between the two methods and provide implementation guidelines.

Mobile communications antennas come in a variety of configurations but are often small with respect to wavelength, consist of thin wires, or have low-profile surfaces. $[Z]$ matrix and $[Y]$ matrix interpolation have been applied to the performance analysis of the antennas shown in Fig. 2. The planar inverted F antenna (PIFA) is a compact low-profile antenna that can be readily integrated onto portable and mobile radios. The circular helix is a thin-wire antenna that is suitable for satellite communications applications. The forked monopole is a unique wire antenna that displays both a monopole resonance and a high-Q transmission line mode resonance. The antenna examples have different numbers of unknowns from one another, which provides some useful insight when comparing computational efficiency.

Section II outlines the MoM formulation used in this paper and describes the $[Z]$ matrix and $[Y]$ matrix interpolation methods. The results of applying the method to several distinctly different mobile communications antennas are presented in Section III. Section IV compares the computational efficiency of both interpolation methods. Section V gives guidelines on the implementation of the methods. Section VI summarizes and concludes the results.

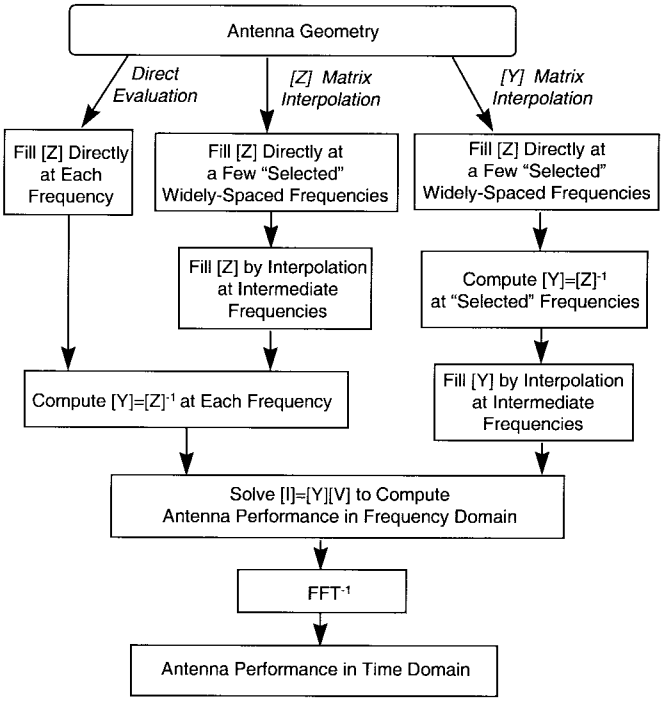

Fig. 1. Comparison of $[Z]$ and $[Y]$ matrix interpolation methodologies.

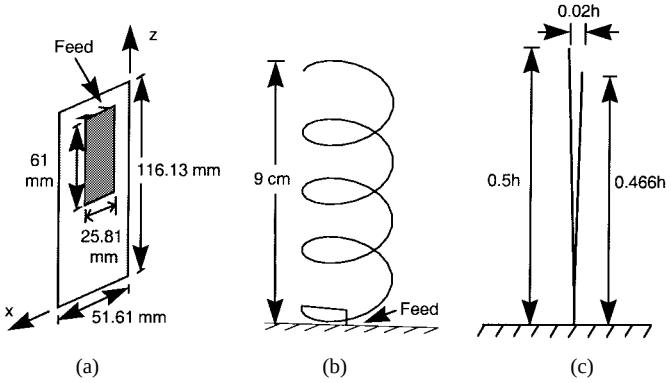

Fig. 2. Antennas for the application of $[Z]$ and $[Y]$ matrix interpolation. (a) PIFA (527 unknowns). (b) Circular helix (88 unknowns). (c) Forked monopole (22 unknowns).

II. Interpolation Methodologies

A. Triangular Surface-Patch Method of Moments Methodology

In the triangular surface-patch MoM formulation for antenna radiation problems, the antenna surfaces are partitioned into N sufficiently small subsections. From this, one sets up and solves the system of equations $[Z][I] = [V]$ to determine the N surface currents on the antenna, where $[Z]$ is the $N \times N$ impedance matrix, $[I]$ is the $N \times 1$ current coefficient

matrix to be determined, and $[V]$ is the $N \times 1$ voltage or excitation matrix. Alternatively, the N surface currents can be determined using $[I] = [Y][V]$, where $[Y]$ is the $N \times N$ admittance matrix that is computed by $[Y] = [Z]^{-1}$.

The formulation described in this paper uses the electric field integral equation (EFIE) for perfect electric conductors (PEC). Using this condition and expressing the total radiated field in terms of potential functions allows one to write

$$[j\omega\vec{A}(\vec{r}) + \nabla\Phi(\vec{r})]_{\tan} = \vec{E}^i_{\tan}(\vec{r}) \tag{1}$$

where

$$\vec{A}(\vec{r}) = \frac{\mu}{4\pi} \int_S \vec{J}(\vec{r}\,') \frac{e^{-jkR}}{R}\, dS' \tag{2}$$

and

$$\Phi(\vec{r}) = -\frac{1}{j4\pi\omega\epsilon} \int_S \nabla'_S \cdot \vec{J}(\vec{r}\,') \frac{e^{-jkR}}{R}\, dS' \tag{3}$$

where $R = |\vec{r} - \vec{r}\,'|$ is the distance between the observation point and source point on the PEC surface S, λ is the wavelength $k = 2\pi/\lambda$, and ϵ and μ are the permittivity and permeability, respectively, of the medium. In this formulation an $e^{j\omega t}$ time convention is used, where $\omega = 2\pi f$ and f denotes the frequency.

In the triangular surface-patch methodology three different linearly independent vector basis functions are used to represent the currents on the antenna. The basis functions depend only upon the geometrical parameters of the particular subsection under consideration. The details of the efficient numerical implementation of the method are discussed in [4] and [5]. Significant computational effort is required to fill the N^2 elements of the $[Z]$ matrix. This effort increases when techniques such as higher order basis functions [16]–[17], are used.

Equations (1)–(3) and the form of the basis and testing functions determine the frequency characteristics of the elements of the $[Z]$ matrix. These equations reveal that the term e^{-jkR} dominates the frequency behavior of the $[Z]$ elements. For matrix element Z_{mn}, R equals $r_{mn} = |\vec{r}_m - \vec{r}_n|$ where $\vec{r}_m$ is the observation location (or subsection) and $\vec{r}_n$ is the source location (or subsection.) When the observation and source are close to each other, r_{mn} is small and $e^{-jkr_{mn}}$ varies slowly with frequency. When they are far from each other, r_{mn} is large and $e^{-jkr_{mn}}$ fluctuates rapidly with frequency. The behavior of the elements of $[Y]$ is not directly discernible from (1)–(3) since the $[Y]$ matrix elements for a particular antenna configuration are only determined after inverting the overall $[Z]$ matrix.

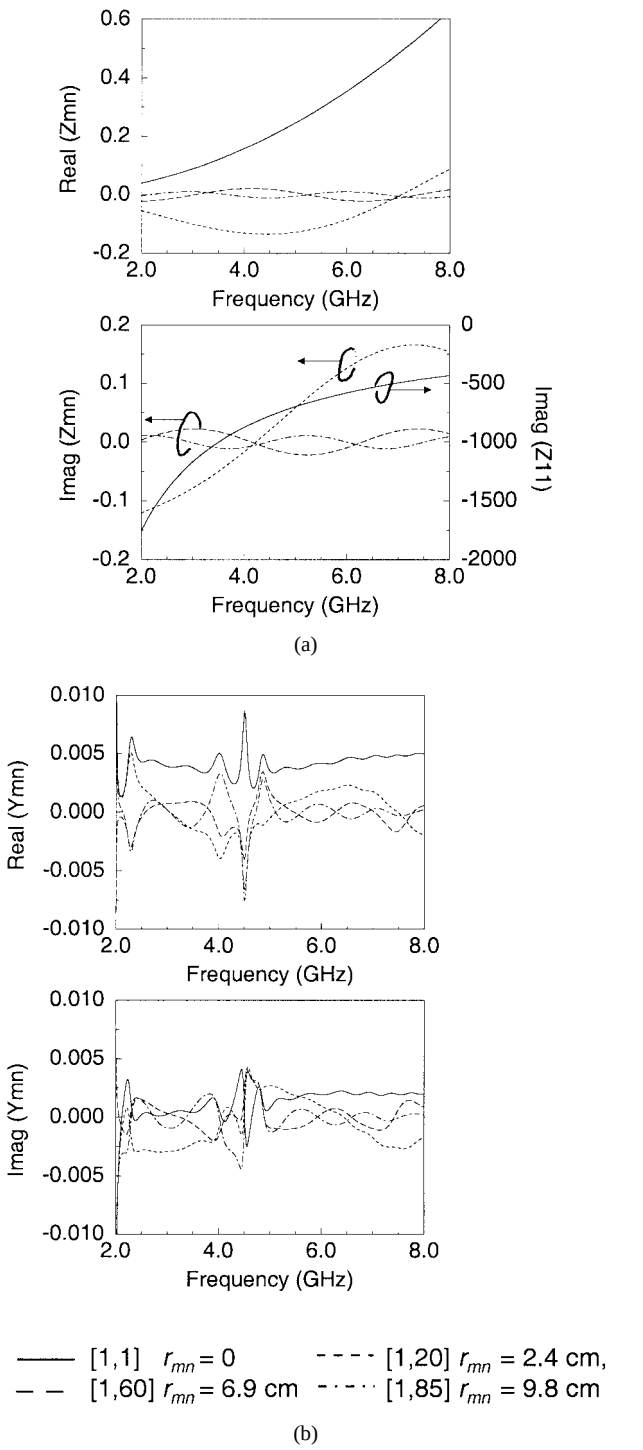

Fig. 3. Comparison of various $[Z]$ and $[Y]$ matrix elements for circular helix. (a) $[Z]$ matrix elements. (b) $[Y]$ matrix elements.

B. Characteristics of $[Z]$ Matrix and $[Y]$ Matrix Elements

Some $[Z]$ matrix and $[Y]$ matrix elements for the helix have been plotted as a function of frequency. Fig. 3 gives a close look at the behavior of some of the $[Z]$ matrix and $[Y]$ matrix elements for the helix for a 4:1 frequency band. $[Z]$ matrix and $[Y]$ matrix elements for small, medium, and large values of r_{mn} are considered. The circular helix has 88 subsections that are numbered from one, located at the attachment point of the antenna and ground plane consecutively to 88, located at the open end of the wire.

The $[Z]$ matrix elements in Fig. 3(a) vary slowly with frequency while the $[Y]$ matrix elements in Fig. 3(b) fluctuate rapidly with frequency. While the elements of the $[Z]$ matrix are practically unaffected by the resonant characteristics of the antenna, the elements of the $[Y]$ matrix are strongly influenced by the resonant behavior. An individual $[Z]$ matrix

element depends only upon the relative spacing between two subsections, whereas the elements of $[Y]$ strongly depend upon the *overall* behavior of the entire antenna structure.

The elements of $[Z]$ can be evaluated over a frequency range by rather simple and low-order interpolation functions, such as a quadratic polynomial. The interpolation of the elements of $[Y]$ over a frequency range requires interpolation functions such as the ratio of two nth order polynomials to accurately capture the frequency behavior of the $[Y]$ matrix elements.

C. $[Z]$ Matrix Interpolation with Quadratic Interpolation Functions

The $[Z]$ matrix interpolation process begins by partitioning the entire frequency band of interest into steps and defining several "selected" frequencies. The interval between adjacent "selected" frequencies defines the interpolation frequency step size. The $[Z]$ matrices for the first three selected frequencies are directly computed by evaluating the potential integrals (2) and (3) as prescribed by the MoM. The elements of $[Z]$ for the intermediate frequencies are approximated by a quadratic function

$$Z_{mn}(f) = A_{mn}f^2 + B_{mn}f + C_{mn} \tag{4}$$

where f denotes frequency and A_{mn}, B_{mn}, and C_{mn} are the mnth elements of the complex coefficient matrices $[A], [B]$, and $[C]$. Equation (4) can be cast into a system of three equations and three unknowns. These equations along with the elements of the directly computed $[Z]$ matrices calculated at three selected frequencies are used to determine the coefficient matrices. If the frequency band of interest is especially wide, it may be necessary to divide the band into several interpolation frequency ranges and implement a process of stepping through them. Quadratic interpolation works best for antennas with surfaces that are smaller than 0.5λ.

The interpolation function can be improved upon by incorporating the frequency behavior of the elements of $[Z]$ into the process [15], [18]. This is done to increase the accuracy in evaluating the terms of $[Z]$ at the intermediate frequencies or allow larger interpolation frequency ranges.. For large antennas, the rapid frequency variation of the factor $e^{-jkr_{mn}}$ dominates the frequency variation of the $[Z]$ matrix elements with large r_{mn}. The quantity

$$Z'_{mn} = \frac{Z_{mn}}{e^{-jkr_{mn}}} \tag{5}$$

varies quite slowly with frequency. When r_{mn} is large with respect to λ, the improved computation of Z_{mn} is evaluated in two steps. First, a Z'_{mn} element is computed by quadratic interpolation using the corresponding elements of the directly computed $[Z']$ matrices. The matrix element Z_{mn} is then determined by multiplying the resultant value by the known factor $e^{-jkr_{mn}}$. The interpolation function can also be cast in a form that accurately models the behavior of the singular and closely spaced terms of $[Z]$. This has been implemented for thin wire antennas [15].

D. $[Y]$ Matrix Interpolation with Ratio of Polynomials Interpolation Functions

Each element of the $[Y]$ matrix is approximated by the ratio of two polynomials given as

$$Y_{mn}(f) = \frac{a_{0,mn} + a_{1,mn}f + a_{2,mn}f^2 + \cdots + a_{p,mn}f^p}{1 + b_{1,mn}f + b_{2,mn}f^2 + \cdots + b_{d,mn}f^d} \tag{6}$$

where f denotes frequency, p denotes the order of the numerator polymonial, d denotes the order of the denominator polynomial, and $a_{0,mn}, a_{1,mn}, \cdots, a_{p,mn}$ and $b_{1,mn}, b_{2,mn}, \cdots, b_{d,mn}$ are the mnth elements of the complex coefficient matrices $[a_0], [a_1], \cdots, [a_p]$ and $[b_1], [b_2], \cdots, [b_d]$, respectively. When the numerator and denominator have the same or nearly the same degree, the ratio of polynomials representation of matrix element Y_{mn} is often better than a polynomial approximation [19]. In this approach, $p + d + 1$ coefficient matrices are computed.

The $[Y]$ matrix interpolation process begins by defining the order of the polynomials in (6). From this, $p+d+1$ "selected" frequencies within the frequency range are identified. An $N \times N$ $[Y]$ matrix, determined by $[Y] = [Z]^{-1}$ is computed for each "selected" frequency. The elements of these matrices are then used to determine the $p + d + 1$ complex coefficient matrices. The mnth element of each coefficient matrix is then substituted into (6) to compute the corresponding element of the $[Y]$ matrix at each intermediate frequency.

The $[Y]$ matrix elements are highly dependent upon the resonant characteristics of the antenna. The method of improving the interpolation by factoring out the $e^{-jkr_{mn}}$ term does not apply to $[Y]$ matrix interpolation. The choices of the polynomial orders in the numerator and denominator depend upon the proximity of adjacent antenna resonances and the overall evaluation frequency range. Since one typically does not know the location of the resonances beforehand, there is no convenient way to quickly determine the order of the numerator and denominator polynomials. In this paper, the same polynomial order is used for the numerator and the denominator.

III. Application of Interpolation Methods to Antenna Performance Analysis

This section compares the results of employing the $[Z]$ matrix and $[Y]$ matrix interpolation methods to the performance evaluation of complex antennas. The methods are applied to an antenna composed primarily of surfaces (a PIFA), a long wire antenna (a circular helix), and a short wire antenna (a forked monopole). These antennas were chosen since they represent a diverse variety of complex antenna configurations with intricate geometries of wires or wires connected to surfaces.

A. Frequency-Domain Analysis of PIFA Antenna

The $[Z]$ matrix and $[Y]$ matrix interpolation schemes have been applied to the computation of the input impedance of the PIFA. Some design details for PIFA's are given in [20]–[22]. The PIFA, shown in Fig. 2(a), consists of an air-suspended rectangular patch element, a small ground plane, and a shorting

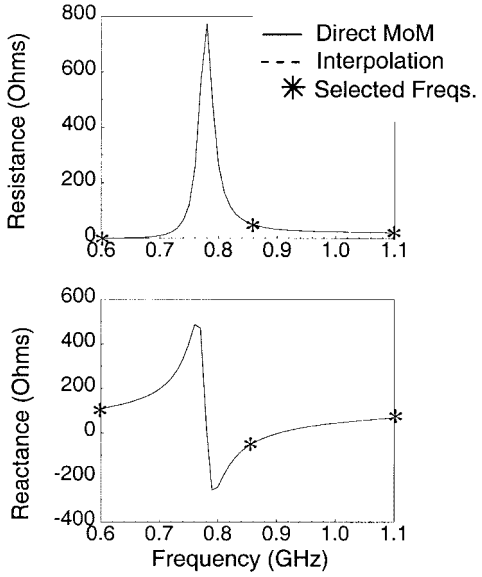

(a)

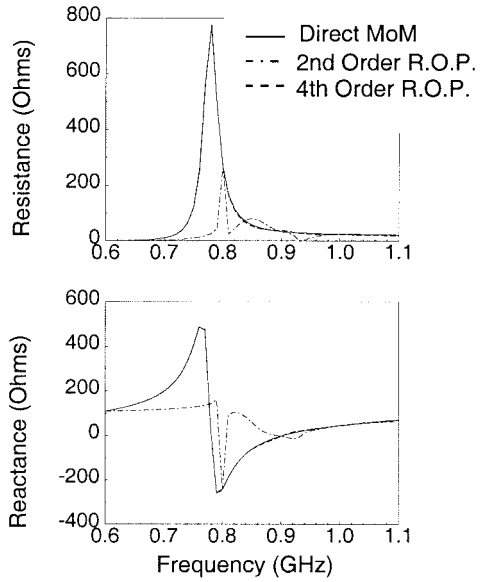

(b)

Fig. 4. Comparison of PIFA input impedance computed by $[Z]$ and $[Y]$ matrix interpolation (in both cases, the data for the dashed and solid lines are superimposed). (a) $[Z]$ matrix interpolation. (b) $[Y]$ matrix interpolation.

plate. The overall mesh consists of 527 unknowns. The antenna is fed by a delta-gap source that is placed between the base of the feed wire and the ground plane.

Fig. 4 compares the input impedance computed by direct MoM, $[Z]$ matrix interpolation, and $[Y]$ matrix interpolation. The input impedance in each case is computed at every 10 MHz. The input impedance computed by quadratic $[Z]$ matrix interpolation uses three selected frequencies located at 0.6, 0.85, and 1.1 GHz. The input impedance computed by $[Y]$ matrix interpolation uses either the ratio of second-order polynomials (second-order R.O.P.) or the ratio of fourth-order polynomials (fourth-order R.O.P). The second-order R.O.P case uses five selected frequencies computed at every 125 MHz. The fourth-order case uses nine selected frequencies computed at every 62.5 MHz.

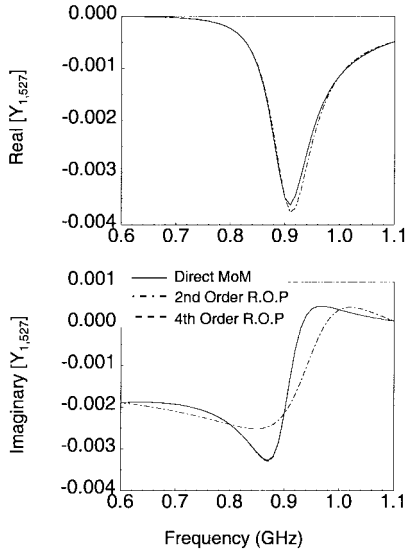

Fig. 5. Comparison of ratio of polynomials representation of matrix element Y_{1527} for PIFA.

Fig. 4(a) shows that the $[Z]$-matrix interpolation results agree well with the direct MoM results. The results for nearly a $2:1$ frequency range are accurately determined by directly computing the MoM $[Z]$ matrix at only three frequencies. $[Z]$ matrix interpolation predicts the resonant behavior at 780 MHz even though there is no selected frequency specifically located at this point. Quadratic $[Z]$ matrix interpolation works well for this antenna because it primarily consists of surface elements and the largest antenna dimension is only 0.43λ at 1.1 GHz.

Fig. 4(b) shows that the $[Y]$ matrix interpolation results computed with fourth-order polynomials agree well with the direct MoM results, while the interpolation results computed with second-order polynomials do not. To understand and explain these results, the ratio of polynomials representation was used to investigate how accurate it can compute a single $[Y]$ matrix element. Fig. 5 shows matrix element $Y_{1,527}$ computed three different ways: 1) by directly inverting the entire $[Z]$ matrix and extracting the $Y_{1,527}$ element at each frequency; 2) by approximating the value of $Y_{1,527}$ by the ratio of second-order polynomials; and 3) by approximating the value of Y_{1527} by the ratio of fourth-order polynomials. The coefficients for the second-order ratio of polynomials were computed by the evaluating $[Y]$ (via the computation and inversion of $[Z]$) at five "selected" frequencies. The coefficients for the fourth-order R.O.P. approximation were computed by evaluating $[Y]$ at nine "selected" frequencies. This figure shows that second-order R.O.P. captures the behavior of the real part of Y_{1527} but does not model the imaginary part very well. The fourth-order R.O.P. accurately determines both the real and imaginary parts of this matrix term. Detailed plots of other $[Y]$ matrix elements show similar comparisons.

Fig. 6 compares the radiation patterns at 0.85 GHz computed directly from MOM, $[Z]$ matrix interpolation, and second-order ratio of polynomials. $[Y]$ matrix interpolation

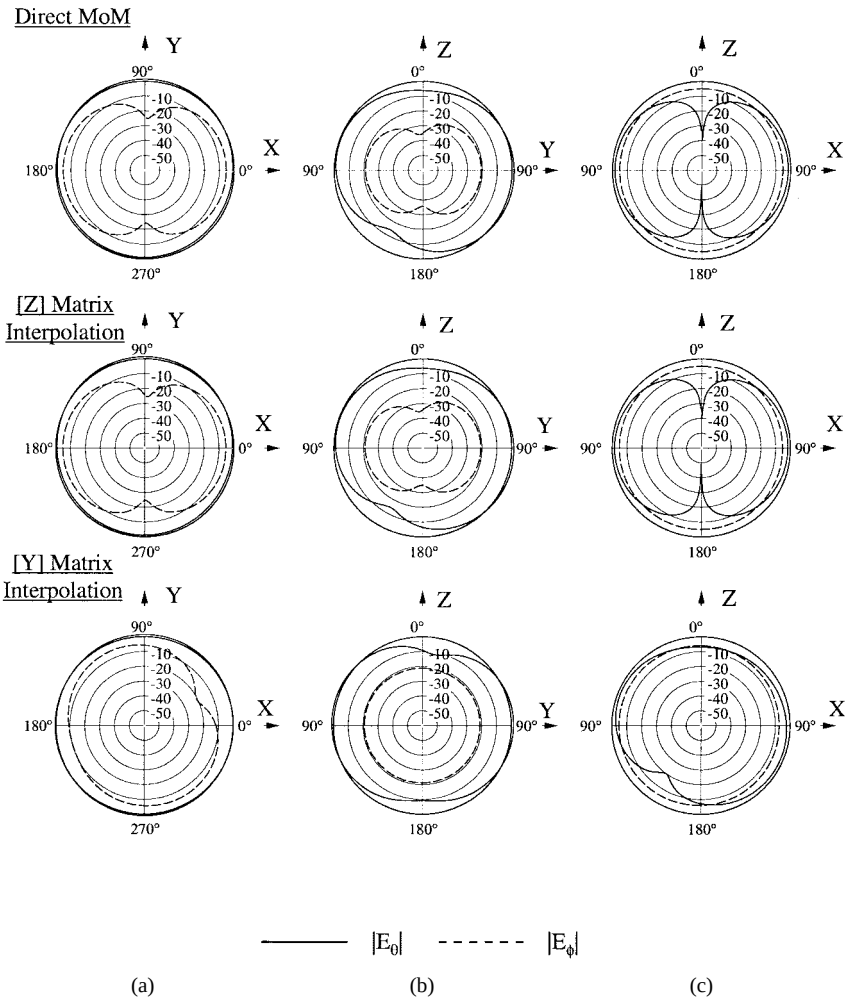

Fig. 6. Comparison of far-field patterns of PIFA at 0.85 GHz computed by $[Z]$ and $[Y]$ matrix interpolation. (a) $|E|$ dB versus $\phi, \theta = 90°$. (b) $|E|$ dB versus $\theta, \phi = 90°$. (c) $|E|$ dB versus $\theta, \phi = 0°$. Selected frequencies for $[Z]$ matrix interpolation are 0.53, 0.78, and 1.03 GHz. Selected frequencies for $[Y]$ matrix interpolation are 0.6, 0.8, 0.9, 1.0, and 1.1 GHz.

using second-order ratio of polynomials. The selected frequencies for $[Z]$ matrix interpolation are 0.53, 0.78, and 1.03 GHz, while the selected frequencies for $[Y]$ matrix interpolation are 0.6, 0.8, 0.9, 1.0 and 1.1 GHz. The patterns computed by the direct MoM and $[Z]$ matrix interpolation agree very well, while the patterns computed using $[Y]$ matrix interpolation do not. When $[Y]$ matrix interpolation is used to compute the radiation patterns at 0.90 GHz (a selected frequency), there is good agreement with the direct MoM results as expected. These results indicate that $[Z]$ matrix interpolation can accurately compute near-field and far-field antenna parameters. They also indicate that higher order polynomials must be used when $[Y]$ matrix interpolation is employed for near-field (input impedance) as well as far-field (radiation patterns) quantities.

B. Frequency-Domain Analysis of Circular Helix

The $[Z]$ matrix and $[Y]$ matrix interpolation schemes were used to the compute the input impedance of a four turn circular helix antenna on an infinite ground plane shown in Fig. 2(b). The helix is in the axial mode near 3 GHz. Some general design details for helix antennas are discussed in [23]. The helix is an excellent candidate to test the interpolation strategies, since the input impedance of this antenna changes quite rapidly at frequencies when additional modes propagate on the antenna. The model for this antenna uses 88 wire subsections and is fed by a delta-gap source located at the base of helix.

The input impedance computed by direct MoM and by $[Z]$ matrix and $[Y]$ matrix interpolation is compared in Fig. 7. Note the rapidly changing input impedance behavior from the additional modes that propagate on the helical structure. The input impedance in each case is computed and plotted at every 20 MHz. The $[Z]$ matrix interpolation frequency step size is 150 MHz. The selected frequencies used for $[Z]$ matrix interpolation are denoted by the five stars "$*$." The impedance computed by $[Z]$ matrix interpolation is calculated by interpolation over the entire $4:1$ frequency band using only five directly computed $[Z]$ matrices, i.e., three subbands are used. The input impedance computed by $[Y]$ matrix interpolation uses either the ratio of fourth-order polynomials (fourth-order R.O.P.) or the ratio of tenth order polynomials

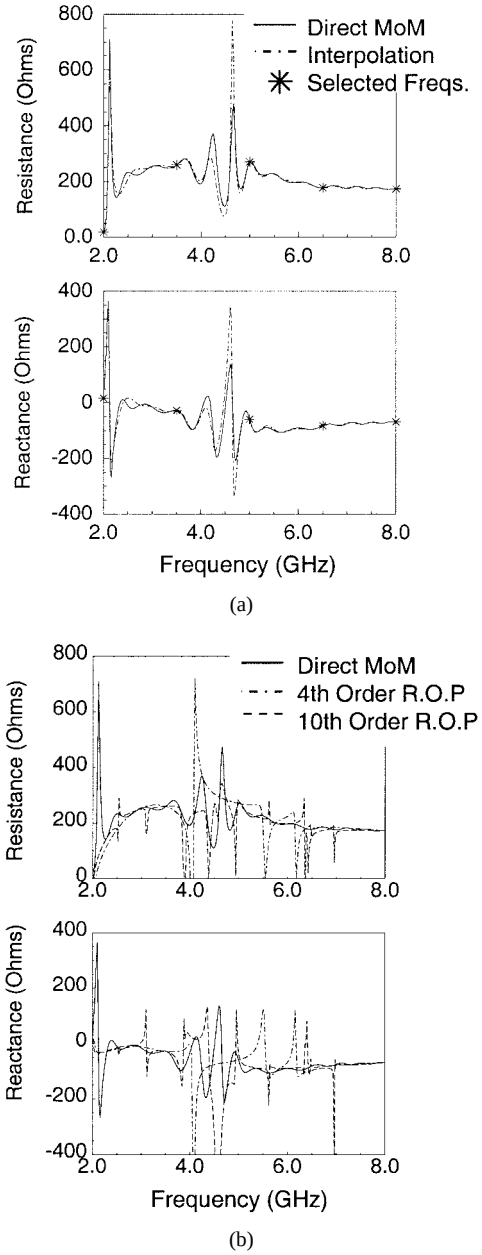

Fig. 7. Comparison of helix input impedance computed by $[Z]$ and $[Y]$ matrix interpolation. (a) $[Z]$ matrix interpolation. (b) $[Y]$ matrix interpolation.

(tenth-order R.O.P). Nine selected frequencies are used for the fourth-order R.O.P case, while 21 selected frequencies are used for the tenth-order R.O.P case. The selected frequencies in each case were chosen by dividing the 2–8 GHz frequency range in equal frequency increments.

The input-impedance behavior of the helix is well modeled with $[Z]$ matrix interpolation. Even the rapid impedance variations between 4 and 5 GHz only slightly differ from the directly computed results. This is significant since the closest selected frequencies are at 3.5 and 5 GHz, which lie outside this range. The $[Y]$ matrix interpolation results show that neither the fourth-order ratio of polynomials nor the tenth-order ratio of polynomials accurately reconstruct the direct MoM input impedance behavior. Higher order polynomials

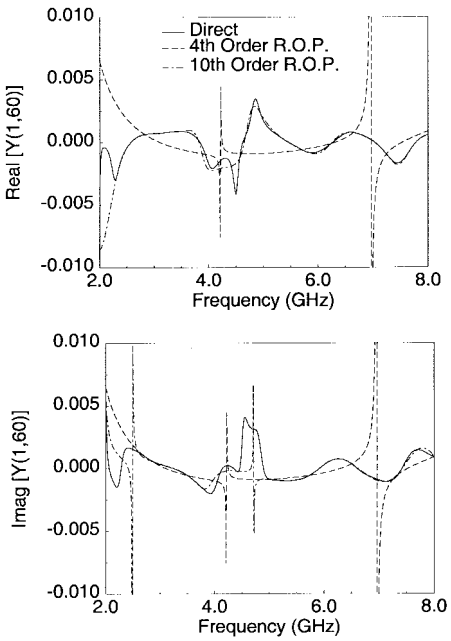

Fig. 8. Comparison of ratio of polynomials representation of matrix element $Y_{1,60}$ for helix.

orders or an efficient scheme to determine different polynomial orders each for the numerator and denominator are needed to accurately predict the input impedance for the entire 4 : 1 band.

A close look at the accuracy of $[Y]$ matrix interpolation for a single helix matrix element for the helix is shown in Fig. 8. This plot compares element $Y_{1,60}$ as a function of frequency computed three different ways: 1) by directly inverting the entire $[Z]$ matrix and extracting the $Y_{1,60}$ element at each frequency; 2) by approximating the value of $Y_{1,60}$ by the ratio of fourth-order polynomials; and 3) by approximating the value of $Y_{1,60}$ by the ratio of tenth-order polynomials, The coefficients for the ratio of fourth-order polynomials. were computed by evaluating $[Y]$ at nine different frequencies. The coefficients for the ratio of tenth-order polynomials were computed by the computing $[Y]$ in the same way at 21 different frequencies. Fig. 8 shows that the ratio of fourth-order polynomials does a rather poor job of reconstructing the real and imaginary parts of this matrix element. The ratio of tenth-order polynomials models most of the detailed features of the real part of $Y_{1,60}$, yet still does not capture many of the features of the imaginary part of $Y_{1,60}$. A ratio of tenth-order polynomials representation for each element of $[Y]$ requires the computation and inversion of $[Z]$ at 21 frequencies as well as the storage of more than 21 [88 $\times$ 88] coefficient matrices. Only five [88 $\times$ 88] coefficient matrices are required to accurately compute the antenna performance with $[Z]$ matrix interpolation.

C. Frequency-Domain Analysis of Forked Monopole

The third comparison pertains to the computation of the input admittance of a forked monopole antenna on an infinite ground plane shown in Fig. 2(c). The forked monopole consists of two “fork” wire segments that are connected together

by a short common segment at the base of the antenna. The forked monopole antenna consists of a basic $\lambda/4$ monopole antenna with an added "forked" element that is slightly shorter than $\lambda/4$. The resultant structure has both a normal mode monopole resonance and a high-Q transmission line mode resonance. This antenna is derived from the bottom-fed fan antenna used by the U.S. Navy for shipboard communications [24]. The MoM geometry model for this antenna consists of two subsections for the short common segment and ten subsections for each "fork" segment. The antenna is fed by a delta-gap source at the base of the common segment. The frequency of the high-Q resonance is determined by the length of the section that is slightly shorter than $\lambda/4$. To resolve the high-Q resonance behavior accurately with discrete frequency samples requires a very small frequency step, thus this antenna is an excellent example to test how well $[Z]$ and $[Y]$ matrix interpolation predict very narrow-band resonances.

Fig. 9 compares the input admittance computed by direct MoM and by $[Z]$ matrix interpolation [using (5)] and by $[Y]$ matrix interpolation. The input admittance in each case is computed at increments of $0.001h/\lambda$. The selected frequencies used in each method are denoted by "$*$." The input admittance computed by $[Z]$ matrix interpolation is calculated over the entire $3:1$ frequency band using only three directly computed $[Z]$ matrices. The input admittance computed by $[Y]$ matrix interpolation uses the ratio of fourth-order polynomials. Since $[Y]$ matrix interpolation with the ratio of lower order polynomials did not accurately compute the input impedance of the PIFA for a $2:1$ frequency band and since the PIFA has much simpler characteristics over the frequency of observation than the forked monopole, lower order polynomials were not used in the $[Y]$ matrix interpolation of the forked monopole.

The input admittance results are similar to the results obtained in Fig. 3 of [24]. The very sharp resonance behavior near $0.72h/\lambda$ is accurately predicted in each case even though no selected frequency is located at this resonance. $[Y]$ matrix interpolation computes the admittance behavior slightly more accurately than $[Z]$ matrix interpolation, yet $[Z]$ matrix interpolation only requires the direct MoM matrix solution for three frequencies.

D. Time-Domain Analysis of Input Current of Circular Helix

One significant advantage of using interpolation to compute the matrix elements is the significant reduction in computation time required to compute the antenna characteristics at the many frequencies needed to calculate the time-domain antenna performance. The flow diagram in Fig. 1 shows how an antenna parameter such as input impedance, computed at many frequencies can be used with an inverse Fourier transform to determine the time-domain antenna behavior.

The $[Z]$ matrix interpolation method has been applied to the analysis of the source current of the circular helix antenna shown in Fig. 2(a) for short-pulse excitation. $[Y]$ matrix interpolation was not employed for this case because of the difficulty in obtaining a high degree of accuracy in computing the input impedance via $[Y]$ matrix interpolation over such a large frequency band.

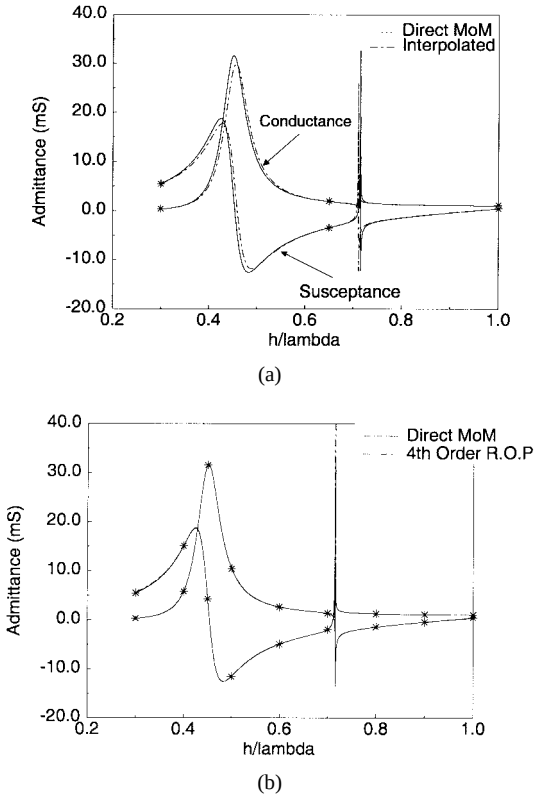

Fig. 9. Comparison of forked monopole input admittance computed by $[Z]$ and $[Y]$ matrix interpolation. "$*$" denotes selected frequencies. (a) Direct MoM and $[Z]$ matrix interpolation. (b) Direct MoM and $[Y]$ matrix interpolation.

The input voltage source is the time derivative of a Gaussian pulse. The temporal behavior of the source voltage impressed at the connection between the base of the helix wire and the infinite ground plane is

$$V_s(t) = 2a^2(t - t_{\max})^2 \exp[-a^2(t - t_{\max})^2] \quad \text{volts} \qquad (7)$$

where $a = 1.5 \times 10^9$ and $t_{\max} = 1.43 \times 10^{-3}$ s. The temporal step size is $\Delta t = 6.26 \times 10^{-11}$ s. Fig. 10 shows the input admittance of the helix as a function of the scaled frequency F/c, where $c = 3 \times 10^8$ m/s. Fig. 10(a) compares the input admittance Y_{in} at 256 frequency points computed by the direct MoM and $[Z]$ matrix interpolation. Fourteen selected frequencies, denoted by "$*$," are used to interpolate the elements of $[Z]$. The input admittance computed by $[Z]$ matrix interpolation agrees well with the values computed by direct MoM since there is a high density of selected frequencies at the lower frequency range. The selected frequencies were chosen by comparing just a few of the elements of the $[Z]$ matrix computed by interpolation and the direct MoM. Since only a few elements were compared and no matrix inversion was involved, this was a quick process. The addition of selected frequencies at the lower frequencies resulted in very good agreement between the directly computed and interpolated matrix elements. The imaginary parts of the elements of $[Z]$ for the self and small r_{mn} terms have a logarithmic variation, rather than a quadratic variation, with frequency. Many selected frequencies were needed at the lower

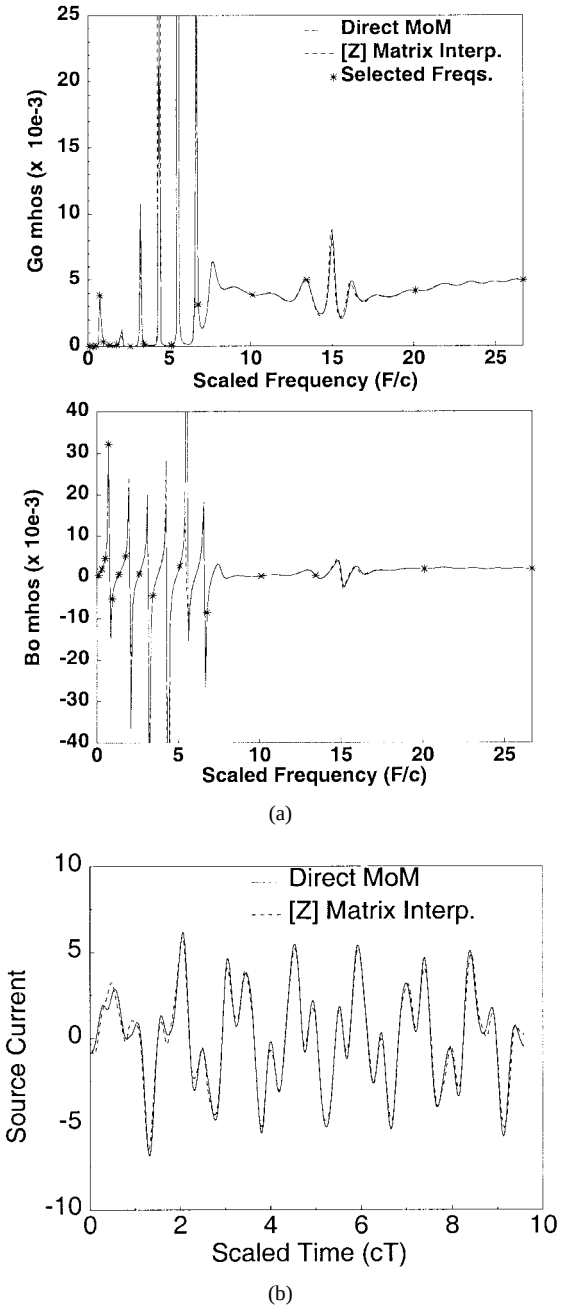

Fig. 10. Time-domain response of source current for helix antenna for time derivative of a Gaussian voltage-source excitation (c is the speed of light). (a) Input admittance. (b) Source current.

frequencies to accurately capture this behavior. Fig. 10(b) compares the time-domain response of the source current computed by direct MoM and by $[Z]$ matrix interpolation.

IV. Comparison of Computational Efficiency

The previous section compared the accuracy of the $[Z]$ matrix and $[Y]$ matrix interpolation for several diverse antenna structures. This section compares the computational efficiency of these methods. $[Z]$ matrix interpolation results in a large time savings over the direct method when the matrix fill time dominates the overall computation time.

TABLE I
Timing Comparison of $[Z]$ and $[Y]$ Matrix Interpolation for PIFA (in CPU Seconds*). 527 Unknowns and 51 Frequencies

	[Z] Fill Directly	[Y] Fill Directly	Coeffs.	[Z] Fill Interp.	[Y] Fill Interp.	Solve	Total
Direct MoM	3050	—	—	—	—	943	3993
[Z] Matrix Interpolation	179.5	—	3.65	82.6	—	943	1208.65
[Y] Matrix Interpolation 2nd Order R.O.P	—	565	72	—	224.50	21	882.5
[Y] Matrix Interpolation 4th Order R.O.P	—	1019	1208	—	372.2	21	2620.2

*IBM RS6000/530H workstation

TABLE II
Timing Comparison of $[Z]$ and $[Y]$ Matrix Interpolation for Helix (in CPU Seconds*). 88 Unknowns and 301 Frequencies

	[Z] Fill Directly	[Y] Fill Directly	Coeffs.	[Z] Fill Interp.	[Y] Fill Interp.	Solve	Total
Direct MoM	1026	—	—	—	—	36	1062
[Z] Matrix Interpolation	17.05	—	0.28	1.45	—	36	53.78
[Y] Matrix Interpolation 4th Order R.O.P	—	32.37	33	—	25.38	1	91.75
[Y] Matrix Interpolation 10th Order R.O.P	—	76.3	46.15	—	56.3	1	179.75

*IBM RS6000/530H workstation

Tables I and II show the computational time used for each of the different steps of the three methods. Table I shows the timing comparison for the PIFA. Three selected frequencies were used for $[Z]$ matrix interpolation, five selected frequencies for $[Y]$ matrix interpolation with second-order ratio of polynomials , and nine selected frequencies for $[Y]$ matrix interpolation with fourth-order ratio of polynomials. Table II shows the timing comparison for the circular helix antenna. Five selected frequencies were used for $[Z]$ matrix interpolation, nine selected frequencies for $[Y]$ matrix interpolation with fourth-order ratio of polynomials, and 21 selected frequencies $[Y]$ matrix interpolation with tenth-order ratio of polynomials.

The first row in these tables shows the total time required to evaluate the surface currents directly with MoM. This time is determined by the time it takes to directly compute and fill all of the N^2 elements of the $[Z]$ matrix and to solve $[Z][I] = [V]$ at each frequency using matrix factorization and decomposition with Linpack subroutines [25]. The second row shows the time involved to compute the surface currents using $[Z]$ matrix interpolation. The total time is determined by the sum of the time it takes to:

1) fill the $[Z]$ matrices directly at the selected frequencies;
2) compute the coefficients of the interpolation functions;

3) fill the $[Z]$ matrices by interpolation at each of the intermediate frequencies;
4) solve for $[I]$ by $[Z][I] = [V]$ at each frequency.

The remaining rows indicate the time required to compute the surface currents using $[Y]$ matrix interpolation. The total time in each $[Y]$ matrix interpolation case is determined by the sum of the time it takes to:

1) compute the $[Y]$ matrices at the selected frequencies;
2) compute the ratio of polynomials coefficients;
3) fill the $[Y]$ matrices by interpolation at the intermediate frequencies;
4) solve for $[I]$ by $[I] = [Y][V]$ at each frequency.

For the PIFA, the direct $[Z]$ matrix fill time per frequency is about three times greater than the solve time. The total computation time using $[Z]$ matrix interpolation is over three times faster than the direct MoM. The total computation time using $[Y]$ matrix interpolation with the ratio of two second-order polynomials is about 4.5 times faster than the direct MoM. This is only a slightly faster than $[Z]$ matrix interpolation. Recall that higher order polynomials are required for the accurate computation of the matrix elements. The computation time with the ratio of two fourth-order polynomials is only about 1.4 times faster than direct MoM. Thus, an accurate simulation utilizing $[Y]$ matrix interpolation may actually take longer than $[Z]$ matrix interpolation.

For the helix, the direct $[Z]$ matrix fill time per frequency is over 28 times greater than the solve time. The overall computation time of the entire frequency sweep using $[Z]$ matrix interpolation is about 19 times greater than the direct MoM. The overall computation time of the frequency sweep using $[Y]$ matrix interpolation with either fourth-order or tenth-order ratio of polynomials is greater than the $[Z]$ matrix interpolation approach.

Next, consider an alternate approach that interpolates the elements of the current—or $[I]$—matrix. Interpolation of the current matrix $[I]$ should be efficient since $[I]$ is only a column matrix of N elements. Table III compares the time required for $[I]$ matrix interpolation for the circular helix. Each element of the $[I]$ matrix is approximated as a ratio of polynomials. Both fourth-order and tenth-order polynomials are considered. The total time in each case is determined by the sum of the time it takes to:

1) compute the $[Y]$ matrices at the selected frequencies;
2) compute the current matrices $[I] = [Y][V]$ at the selected frequencies;
3) compute the ratio of polynomials coefficients;
4) compute the final $[I]$ matrices by interpolation at the intermediate frequencies.

The overall computation time of $[I]$ matrix interpolation with fourth-order ratio of polynomials is less than the time for $[Z]$ matrix interpolation. However, since inadequate accuracy was obtained with this order $[Y]$ matrix interpolation and since the elements of $[I]$ have similar variation as the elements of $[Y]$, higher order polynomials for accurate $[I]$ matrix interpolation are required. The overall computation time of $[I]$ matrix interpolation with the ratio of two tenth-order polynomials is actually *greater* than the time for $[Z]$ matrix interpolation.

TABLE III
COMPARISON OF $[I]$ MATRIX INTERPOLATION FOR HELIX (IN CPU SECONDS*). 88 UNKNOWNS AND 301 FREQUENCIES

	[Y] Fill Directly	Solve	Coeffs. [Nx1]	[I] Fill Interp.	Total
[I] Matrix Interpolation 4th Order R.O.P	32.37	1	0.375	0.28	34.025
[I] Matrix Interpolation 10th Order R.O.P	76.3	1	0.52	0.63	77.43

*IBM RS6000/530H workstation

In addition to comparing the computational run time efficiency, the increase in memory storage must also be considered. Many techniques that serve to reduce the overall simulation time do so at the expense of increased memory storage and, thus, limit the size of the problem that can be run. $[Z]$ matrix interpolation uses four times the memory of the direct Mom approach. In addition to storing the $[Z]$ matrix for the intermediate computation frequency of interest, three matrices for the complex quadratic coefficients must be stored. When the interpolation process is divided into several frequency subbands, two additional direct filled $[Z]$ matrices must also be saved. Since the greatest computation speed up is obtained for $[Z]$ matrices with small or medium order, the storage of all the matrices can typically fit within the computational memory of computer workstations used for method of moments computations.

When second-order polynomials are used, the $[Y]$ matrix interpolation method uses six times the memory of the direct MoM approach. In this case, five coefficient matrices as well as the $[Y]$ matrix for the intermediate computation frequency of interest must be stored. When fourth-order polynomials are used, the memory requirement increases to nine times the memory of the direct MoM approach. The memory requirement is 22 times that of the direct MoM approach when tenth-order polynomials are used.

V. IMPLEMENTATION GUIDELINES

To compute the broad-band frequency performance of the antenna as rapidly as possible, the interpolation frequency step must be carefully chosen. A small interpolation frequency step means that $[Z]$ or $[Y]$ matrices are directly computed and filled for many frequencies. A very large interpolation frequency step results in poor reconstruction of the matrix elements.

To choose a suitable interpolation frequency step size for $[Z]$ matrix interpolation, one can easily review the characteristics of several $[Z]$ matrix elements. A plot of just a few of the elements of $[Z]$ that represent the full span (smallest, largest, and mid range) of r_{mn} values can be used to quickly identify the overall frequency range at which the matrix elements can be accurately fitted by a chosen interpolation function. The overall accuracy obtained from $[Z]$ matrix interpolation is not highly dependent upon the precise location of the

selected frequencies, yet they should be fairly well spaced over the frequency range. The computation time required to compute several $[Z]$ matrix elements is significantly smaller than computing and inverting the overall $[Z]$ matrix. Such an approach can be used to ensure the accuracy of the simulated results without requiring any *apriori* knowledge of the specified antenna resonant behavior.

There is no rapid way to compute a few $[Y]$ matrix elements over the entire frequency band, since the *entire* $[Z]$ matrix must be completely filled and inverted to extract even just a few $[Y]$ matrix elements. Thus, there is no convenient way to assess the order of the polynomials to use for $[Y]$ matrix interpolation. The choice of the order is highly dependent upon the resonant nature of the structure which can be quite difficult to determine beforehand.

VI. Conclusions

The $[Z]$ matrix interpolation and $[Y]$ matrix interpolation methodologies have been used with the method of moments in order to significantly reduce the computation time required for the wide-band performance evaluation of antennas. Both methods compute the overall surface currents on the antenna that can then be used to evaluate the antenna pattern or input impedance. These interpolation methods do not require the *a priori* knowledge of antenna resonances.

The utility of the methods has been illustrated by their application to different types of antennas used for mobile communications antennas. The examples represent a diversity of antenna types with different size matrices. The results show that the $[Z]$ matrix interpolation method is robust to antenna geometry, the choice of the selected frequencies, and can predict narrow-band resonances. The results show that $[Y]$ matrix interpolation, on the other hand, is highly dependent upon the resonant characteristics of the particular antenna structure.

The work included a comparison of the time savings of both the interpolation methods over the direct MoM approach. When low-order polynomial functions are used in $[Y]$ matrix interpolation, it has the time advantage over $[Z]$ matrix interpolation. However, when large-order polynomials are required to accurately reproduce the elements via $[Y]$ matrix interpolation, then $[Z]$ matrix interpolation is faster. Higher order polynomials for $[Y]$ matrix interpolation requires the storage of more coefficients than $[Z]$ matrix interpolation and requires more computation time.

The advantage of one interpolation method over the other is based upon the general resonant nature of the antenna to be modeled. When many resonances occur within a particular frequency range, $[Z]$ matrix interpolation is faster and requires less computational resources. When there are only one or two resonances within a particular range, $[Y]$ matrix interpolation is more efficient. The results presented in this paper demonstrate the wide range of applicability of the matrix interpolation methods. It was stated from the outset of this work that the key advantage of these interpolation methods is their ability to be easily linked with an existing MoM program. Thus, these interpolation methods can be applied to a wide variety of MoM problems that utilize similar Green's functions or integral equations.

References

[1] M. A. Jensen and Y. Rahmat-Samii, "Performance analysis of antennas for hand-held transceivers using FDTD," *IEEE Trans. Antennas Propagat.*, vol. 42, pp. 1106–1113, Aug. 1994.

[2] Y. Rahmat-Samii and M. A. Jensen, "Characterization of antennas for personal wireless communications applications," *Int. J. Wireless Inform. Networks*, vol. 1, pp. 165–175, 1994.

[3] S. M. Rao, D. R. Wilton, and A. W. Glisson, "Electromagnetic scattering by surfaces of arbitrary shape," *IEEE Trans. Antennas Propagat.*, vol. AP-30, pp. 409–418, May 1982.

[4] S.-U. Wu and D. R. Wilton, "Electromagnetic scattering and radiation by arbitrary configurations of conducting bodies and wires," Tech. Document 1325, Appl. Electromagn. Lab., Dept. Elect. Eng., Univ. Houston, TX, Aug. 1988.

[5] R. E. Hodges and Y. Rahmat-Samii, "An iterative current-based hybrid method for complex structures," *IEEE Trans. Antennas Propagat.*, vol. 45, pp. 265–276, Feb. 1997.

[6] J. S. Colburn and Y. Rahmat-Samii, "Evaluation of personal communications dual-antenna handset diversity performance," *IEEE Trans. Veh. Technol.*, vol. 47, pp. 737–746, Aug. 1998

[7] T. K Sarkar, K. R. Siarkiewicz, and R. F. Stratton, "Survey of numerical methods for solution of large systems of linear equations for electromagnetic field problems," *IEEE Trans. Antennas Propagat.*, vol. AP-29, pp. 847–856, Nov. 1981.

[8] F. X. Canning, "Direct solution of the EFIE with half the computation," *IEEE Trans. Antennas Propagat.*, vol. 39, pp. 118-119, Jan. 1991.

[9] G. F. Herrmann, "Note on interpolational basis functions in the method of moments," *IEEE Trans. Antennas Propagat.*, vol. 38, pp. 134–137, Jan. 1990.

[10] T. W. Nuteson, K. Naishadham, and R. Mittra, "Spatial interpolation of the moment matrix in electromagnetic scattering and radiation problems," in *IEEE Antennas Propagat. Soc. Int. Symp. Dig.*, Ann Arbor, MI, June 1993, pp. 860–863.

[11] G. Vecchi, P. Pirinoli, L. Matekovits, and M. Orefice, "Reduction of the filling time of method of moments matrices," in *11th Annu. Rev. Progress Appl. Computat. Electromagn.*, Monterey, CA, Mar. 1995, pp. 600-605.

[12] G. J. Burke, E. K. Miller, S. Chakrabarti, and K. Demarest, "Using model-based parameter estimation to increase the efficiency of computing electromagnetic transfer functions," *IEEE Trans. Magn.*, vol. 25, pp. 2807–2809, July 1989.

[13] K. Kottapalli, T. K. Sarkar, Y. Hua, E. K. Miller, and G. J. Burke, "Accurate computation of wide-band response of electromagnetic systems utilizing narrow-band information," *IEEE Trans. Microwave Theory Tech.*, vol. 39, pp. 682–687, Apr. 1991.

[14] E. H. Newman and D. Forrai, "Scattering from a microstrip patch," *IEEE Trans. Antennas Propagat.*, vol. AP-35, pp. 245-251, Mar. 1987.

[15] E. H. Newman, "Generation of wide-band data from the method of moments by interpolating the impedance matrix," *IEEE Trans. Antennas Propagat.*, 36, pp. 1820–1824, Dec. 1988.

[16] A. F. Peterson,"Higher-order surface patch basis functions for EFIE formulations," in *IEEE Antennas Propagat. Soc. Int. Symp. Dig.*, Seattle, WA, June 1994, pp. 2162–2165.

[17] D. R. Wilton, "Review of current status and trends in the use of integral equations in computational electromagnetics," *Electromagn.*, vol. 12, pp. 287–341, 1992.

[18] K. L. Virga and Y. Rahmat-Samii, "Generation of wideband antenna performance by $[Z]$ and $[Y]$ matrix interpolation in the method of moments," in *Ultra-Wideband Short Pulse Electromagnetics III.* New York: Plenum, 1996.

[19] R. L. Burden and J. D. Faires, *Numerical Analysis*, 5th ed. Boston, MA: PWS-Kent, 1988, ch. 8.

[20] T. Taga and K. Tsunekawa, "Performance analysis of a built-in inverted F antenna for 800 Mhz band portable radio units," *IEEE J. Select. Areas Commun.*, vol. SAC-5, pp. 921–929, June 1983.

[21] K. Hirasawa and M. Haneishi, *Analysis, Design and Measurement of Small Low Profile Antennas*. Norwood, MA: Artech House, 1992.

[22] K. Virga and Y. Rahmat-Samii, "Low-profile enhanced-bandwidth PIFA antennas for wireless communications packaging," *IEEE Trans. Microwave Theory Tech.*, vol. 45, pp. 1879–1888, Oct. 1997.

[23] J. D. Kraus, *Antennas*. New York: McGraw-Hill, 1988.

[24] G. J. Burke and A. J. Poggio, "Computer Analysis of the Bottom-Fed Fan Antenna," UCRL-52109, Lawrence Livermore Lab., Univ. California, Livermore, Aug. 1976.

[25] J. J. Dongarra, *Linpack User's Guide*. Philadephia, PA: Soc. Indust. Appl. Math., 1979.

Kathleen L. Virga (S'84–M'95–SM'97) received the B.S. degree from California State University, Long Beach, in 1985, the M.S. degree from California State University, Northridge, in 1987, and the Ph.D. degree from the University of California, Los Angeles (UCLA), in 1996, all in electrical engineering.

From 1985 to 1996, she worked in the Radar Systems Group, Hughes Electronics, Electromagnetic Systems and Solid-State Microwave Laboratories. She has been a Task Leader and Supervisor for several internal research and development projects. She is currently an Assistant Professor in the Electrical and Computer Engineering Department at the University of Arizona, Tucson. Her experience includes the design and development of phase shifters, RF feed networks, radiator elements, and tranmit/receive modules for airborne phased-array and active-array antennas for which she holds four patents.She is the Associate Editor responsible for the professional activities (PACE) column in the *Antenna and Propagation Society Magazine*. Her current research interests include mobile communications, conformal antenna arrays, and the design and measurements of high-density packaging for high-speed digital and microwave applications.

Dr. Virga is a member of Eta Kappa Nu, Tau Beta Pi, Sigma Xi, and the IEEE Antennas and Propagation (AP-S) and Microwave Theory and Techniques (MTT) Societies. She serves as the PACE chair for the AP-S Society. She served on the Steering Committee that hosted the 1994 MTT International Microwave Symposium and the Technical Program Committee for the 1998 AP-S Symposium. In 1996, she was the second-place finalist in the USNC-URSI Student Paper Competition and received the UCLA Department of Electrical Engineering Graduate Woman of the Year Award. She was the invited keynote speaker for the 1996 California State University Northridge, School of Engineering commencement.

Yahya Rahmat-Samii (S'73–M'75–SM'79–F'85) received the M.S. and Ph.D. degrees in electrical engineering from the University of Illinois, Urbana-Champaign.

He was a Senior Research Scientist at NASA's Jet Propulsion Laboratory/California Institute of Technology. In 1986, he was a Guest Professor at the Technical University of Denmark (TUD). He has been a consultant to many aerospace companies. He is currently Professor of electrical engineering at the University of California at Los Angeles (UCLA). He has authored and coauthoreed over 400 technical journal articles and conference papers, has written 14 book chapters, and is the coauthor of *Impedance Boundary Conditions in Electromagnetics* (Washington, DC: Taylor Francis, 1995). He has been the editor and guest editor of many technical journals and book publications. He also the holds several patents. His research contributions cover a diverse area of electromagnetics, antennas, measurement and diagnostic techniques, numerical and asymptotic methods, and satellite and personal communications.

Dr. Rahmat-Samii is a Fellow of IAE, a member or Commissions A, B, and J of USNC/URSI, AMTA, Sigma Xi, Eta Kappa Nu, and the Electomagnetics Academy. He was the 1995 President of the IEEE Antennas and Propagation Society, and was appointed an IEEE Antennas and Propagation Society Distinguished Lecturer. He has been the guest and plenary session speaker at many national and international symposia, was one of the directors and vice president of the Antennas Measurement Techniques Association (AMTA) for three years, and was a member of UCLA's graduate council. He received numerous NASA and JPL Certificates of Recognition. In 1984, he was the recipient of the prestigious Henry Booker Award of URSI. In 1992 and 1995, he was the recipient of the Best Application Award (Wheeler Award) for papers published in the IEEE TRANSACTIONS ON ANTENNAS AND PROPAGATION. He is listed in *Who's Who in America, Who's Who in Frontiers of Science and Technology*, and *Who's Who in Engineering*.